




**Direct numerical simulations of turbulent pipe flow at high Reynolds number**A. Ceci \* and S. Pirozzoli*Dipartimento di Ingegneria Meccanica e Aerospaziale, Sapienza Università di Roma,  
Via Eudossiana 18, 00184 Roma, Italy*J. Romero  and M. Fatica *NVIDIA Corporation, 2701 San Tomas Expressway, Santa Clara, California 95050, USA*

R. Verzicco

*Dipartimento di Ingegneria Industriale, Università di Roma Tor Vergata,  
Via del Politecnico 1, 00133 Roma, Italy  
and Physics of Fluid Group, University of Twente, PO Box 217, 7500 AE Enschede, Netherlands*

P. Orlandi

*Dipartimento di Ingegneria Meccanica e Aerospaziale, Sapienza Università di Roma,  
Via Eudossiana 18, 00184 Roma, Italy*

(Received 28 June 2022; published 7 November 2022)

This paper is associated with a video winner of a 2021 American Physical Society's Division of Fluid Dynamics (DFD) Gallery of Fluid Motion Award for work presented at the DFD Gallery of Fluid Motion. The original video is available online at the Gallery of Fluid Motion, <https://doi.org/10.1103/APS.DFD.2021.GFM.V0053>.

DOI: [10.1103/PhysRevFluids.7.110510](https://doi.org/10.1103/PhysRevFluids.7.110510)

Flow in circular pipes is paradigmatic in the study of fluid turbulence. For compelling practical reasons, it was considered since pioneering studies dealing with hydraulic engineering [1], in which it continues to play a prominent role. Pipe flow was also the subject of the landmark study of Reynolds [2], which first highlighted the importance of what was later called the Reynolds number in determining the passage from a direct to a sinuous regime. Pipe flow was considered by Nikuradse [3] in the first systematic study of the effect of coarse and fine roughness on resistance as a function of the Reynolds number. Because of its theoretical and practical importance, pipe flow has been studied in modern experimental facilities, such as the Princeton Superpipe pressurized facility [4–6] and the CICLOPE facility of the University of Bologna [7,8], which however suffer from problems in accessing the near-wall layer. Direct numerical simulations (DNSs) are a better candidate than experiments to provide high-quality visualizations of turbulent flow. Direct numerical simulations of pipe flow have been numerous, although not as many as for channel flow, and include a number of notable works [9–13].

In a recent paper [14] the present authors first reported DNS results of pipe flow at friction Reynolds number from  $Re_\tau \approx 180$  to  $Re_\tau \approx 6000$  [here  $Re_\tau = u_\tau R/\nu$ , with  $u_\tau = (\tau_w/\rho)^{1/2}$  the

\*alessandro.ceci@uniroma1.it

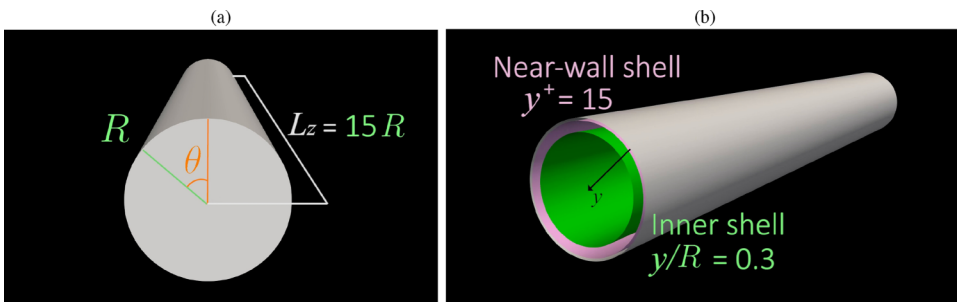


FIG. 1. Pipe geometry: (a) coordinate system and typical length scales and (b) location of reference shells used in the flow visualizations.

friction velocity,  $R$  the pipe radius,  $\tau_w$  the wall shear stress, and  $\rho$  and  $\nu$  the fluid density and kinematic viscosity]. Rendering and animations of the flow field computed from the DNS database of Pirozzoli *et al.* [14] have been generated by using the open-source cinematic package BLENDER [15] and the visualization toolkit PARAVIEW [16]. Full automation of the process of animation generation has been achieved by means of the PVPYTHON backend. The numerical simulations are carried out in a domain with axial length  $15R$  [see Fig. 1(a)]. In the figure we also show for reference two cylindrical shells corresponding to a near-wall position  $y^+ \approx 15$  ( $y = R - r$  is the distance from the wall and the plus superscript denotes normalization with wall units  $u_\tau$  and  $\nu$ ) and farther from it, namely,  $y/R = 0.3$ .

The instantaneous axial velocity field at  $\text{Re}_\tau = 6000$  is shown in Fig. 2. The flow in the cross-stream plane [Fig. 2(a)] features a limited number of bulges distributed along the azimuthal direction, which correspond to alternating intrusions of high-speed fluid from the pipe core and ejections of low-speed fluid from the wall. As in all canonical wall-bounded flow, flow-aligned streaks are visible in the near-wall cylindrical shell [17]. The organization of the streaks is clearly on two different length scales: On top of a sea of tiny streaks, larger zones with velocity higher than the mean (in red) and lower than the mean (in blue) are visible, which are elongated along the axial direction and whose size is comparable to the pipe radius.

Additional information about the large-scale streaks, which are referred to as very-large-scale motions [18], is provided in Fig. 3, where we show axial velocity contours in the two reference cylindrical shells, after unrolling for ease of interpretation. Scale separation between small- and

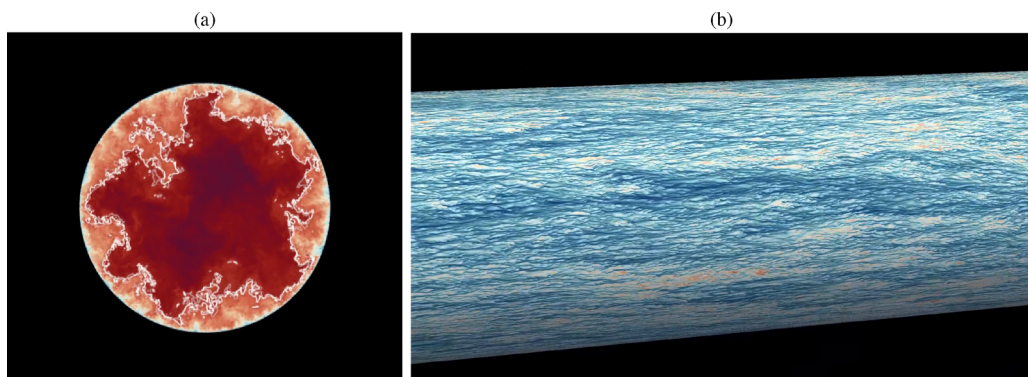


FIG. 2. DNS of pipe flow at  $\text{Re}_\tau = 6000$ : instantaneous axial velocity field (a) in a cross-stream plane and (b) at  $y^+ \approx 15$ . The color scale ranges from 0 (blue) to  $1.3u_b$  (red) and the white isoline in (a) marks the isolevel  $u_z/u_b = 0.9$ .

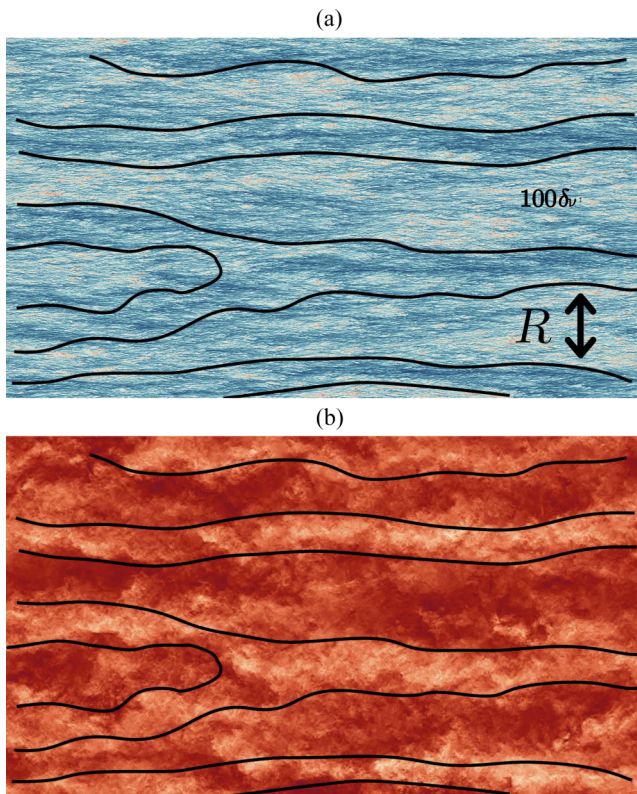


FIG. 3. DNS of pipe flow at  $Re_\tau = 6000$ : instantaneous axial velocity field  $u_z/u_b$ , in unrolled cylindrical shells, at (a)  $y^+ = 15$  and (b)  $y/R = 0.3$ . The color scale ranges from 0 (blue) to  $1.3u_b$  (red).

large-scale streaks is here more clearly visible, with large structures scaling with  $R$  and small ones scaling in wall units. Hand-sketched black lines are used to trace the approximate boundaries of the large-scale high- and low-speed streaks in the near-wall shell, which are also reported in the  $y/R = 0.3$  shell [Fig. 3(b)]. Remarkable association is observed, which proves with little doubt that large-scale near-wall organization results from imprinting of large eddies residing in the core part of the flow [19].

Reynolds number effects are emphasized in Fig. 4, in which we compare DNSs at extreme Reynolds numbers. Figure 4(a) strikingly highlights that, despite the presence of finer details, the flow organization at the large scales at  $Re_\tau = 6000$  is very similar to the case  $Re_\tau = 180$ , both in the near-wall shell and in the core flow. This is corroborated by Fig. 4(b), which shows that the large-scale organization of the velocity field is essentially unaffected by a large change of the Reynolds number. In fact, analysis of the azimuthal spectra shows the dominance of the  $k_\theta = 4$  mode in both cases.

In summary, the flow visualizations reported herein provide strong support for the idea that turbulence in pipe flow results from superposition and interaction of near-wall dynamics occurring on viscous length scales and timescales and of a core flow dynamics whose typical eddies scale on  $R$  and which just like the former is characterized by streamwise leaning streaks which are meandering in the azimuthal directions. This evidence seems to be in support of the scenario envisaged by Dennis and Sogaro [20], based on experimental measurements at lower Reynolds number.

A baseline software supporting the findings of this paper can be found in [21]. The code can also be found in [22].

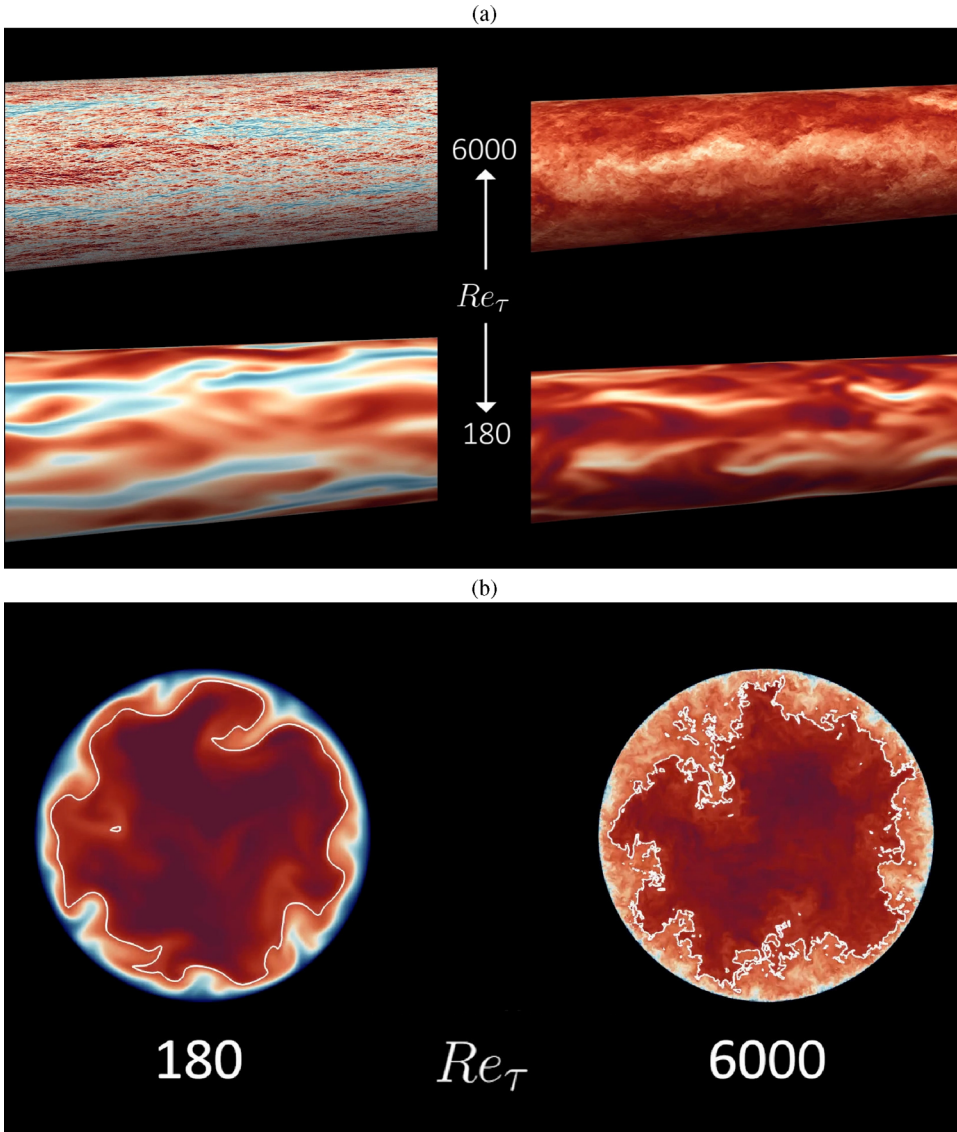


FIG. 4. Comparison of axial velocity fields for DNS at  $Re_\tau = 180$  and 6000: (a) near-wall shell (left) and  $y/R = 0.3$  shell (right) and (b) cross-stream plane.

This work was supported by TEAMAero Horizon 2020 research and innovation program under Grant Agreement No. 860909. We acknowledge that the results reported in this paper were achieved with computational resources under project PRACE No. 2019204979, using the PRACE Research Infrastructure resource MARCONI100 based at CINECA, Casalecchio di Reno, Italy.

- [1] H. Darcy, *Les Fontaines Publiques de la Ville de Dijon* (Dalmont, Paris, 1856).
- [2] O. Reynolds, An experimental investigation of the circumstances which determine whether the motion of water shall be direct or sinuous, and of the law of resistance in parallel channels, *Philos. Trans. R. Soc. London* **174**, 935 (1883).
- [3] J. Nikuradse, Strömungsgesetze in rauhen Röhren, *Forschungsarbeiten auf dem Gebiete des Ingenieurwesens* **361**, 1 (1933).
- [4] M. Zagarola and A. Smits, Mean-flow scaling of turbulent pipe flow, *J. Fluid Mech.* **373**, 33 (1998).
- [5] B. J. McKeon, M. Zagarola, and A. J. Smits, A new friction factor relationship for fully developed pipe flow, *J. Fluid Mech.* **538**, 429 (2005).
- [6] M. Hultmark, S. Bailey, and A. Smits, Scaling of near-wall turbulence in pipe flow, *J. Fluid Mech.* **649**, 103 (2010).
- [7] T. Fiorini, Turbulent pipe flow - High resolution measurements in CICLoPE, Ph.D. thesis, University of Bologna, 2017.
- [8] C. Willert, J. Soria, M. Stanislas, J. Klinner, O. Amili, M. Eisfelder, C. Cuvier, G. Bellani, T. Fiorini, and A. Talamelli, Near-wall statistics of a turbulent pipe flow at shear Reynolds numbers up to 40 000, *J. Fluid Mech.* **826**, R5 (2017).
- [9] J. Eggels, F. Unger, M. Weiss, J. Westerweel, R. Adrian, R. Friedrich, and F. Nieuwstadt, Fully developed turbulent pipe flow: A comparison between direct numerical simulation and experiment, *J. Fluid Mech.* **268**, 175 (1994).
- [10] X. Wu and P. Moin, A direct numerical simulation study on the mean velocity characteristics in turbulent pipe flow, *J. Fluid Mech.* **608**, 81 (2008).
- [11] G. El Khoury, P. Schlatter, A. Noorani, P. Fischer, G. Brethouwer, and A. Johansson, Direct numerical simulation of turbulent pipe flow at moderately high Reynolds numbers, *Flow, Turbul. Combust.* **91**, 475 (2013).
- [12] C. Chin, J. Monty, and A. Ooi, Reynolds number effects in DNS of pipe flow and comparison with channels and boundary layers, *Int. J. Heat Fluid Flow* **45**, 33 (2014).
- [13] J. Ahn, J. Lee, S. Jang, and H. Sung, Direct numerical simulations of fully developed turbulent pipe flows for  $Re_\tau = 180, 544$  and  $934$ , *Int. J. Heat Fluid Flow* **44**, 222 (2013).
- [14] S. Pirozzoli, J. Romero, M. Fatica, R. Verzicco, and P. Orlandi, One-point statistics for turbulent pipe flow up to  $Re_\tau \approx 6000$ , *J. Fluid Mech.* **926**, A28 (2021).
- [15] Blender Online Community, *Blender: A 3D modelling and rendering package* (Blender Foundation, Blender Institute, Amsterdam, 2022), <http://www.blender.org>.
- [16] J. P. Ahrens, B. Geveci, and C. C. Law, ParaView: An end-user tool for large-data visualization, in *The Visualization Handbook* (Elsevier, Amsterdam, 2005).
- [17] S. J. Kline, W. C. Reynolds, W. C. Schraub, and F. A. Runstadler, The structure of turbulent boundary layers, *J. Fluid Mech.* **30**, 741 (1967).
- [18] K. Kim and R. Adrian, Very large-scale motion in the outer layer, *Phys. Fluids* **11**, 417 (1999).
- [19] N. Hutchins and I. Marusic, Evidence of very long meandering features in the logarithmic region of turbulent boundary layers, *J. Fluid Mech.* **579**, 1 (2007).
- [20] D. J. C. Dennis and F. M. Sogaro, Distinct Organizational States of Fully Developed Turbulent Pipe Flow, *Phys. Rev. Lett.* **113**, 234501 (2014).
- [21] A. Ceci, pvpython example for Paraview rendering (Version 1.0), Zenodo (2022), <https://doi.org/10.5281/zenodo.7093373>.
- [22] <http://newton.dma.uniroma1.it/pipe/>.